Transformation Smoothing to use after Positioning of Finite Element Human Body Models

Tomas Janak, Yoann Lafon, Philippe Petit, Philippe Beillas

Abstract While positioning Finite Element Human Body Models is required for many applications, positioning techniques often degrade the mesh quality or result in soft tissues artefacts. This study presents a method to smooth the transformation between two states of the same human body model in an attempt to maintain the initial element quality, conserve gaps between disconnected components and keep bones as rigid. Illustrative workflows are provided for three positioning test cases using either the PIPER positioning tool or a finite element simulation, and either the PIPER Child or the GHBMC M50-O detailed human body model. The workflows describe how to correct surface artefacts such as unrealistic folds or how to remove elements with negative volumes resulting from the PIPER positioning tool, by using a combination of surface smoothing and transformation smoothing. Parameters and performance are discussed to help future applications. The approach requires limited user interaction and produces a smoothed model within a few minutes, in most cases. The transformation smoothing is independent of the positioning approach and the topology of the human body model, making it potentially applicable to multiple scenarios. The method is implemented within the PIPER open source framework.

Keywords finite element, human body models, kriging, positioning, smoothing

I. INTRODUCTION

Changing the posture of finite element (FE) Human Body Models (HBM) such as the Global Human Body Model Consortium (www.ghbmc.com) models or the PIPER Child model (www.piper-project.org) is likely to affect mesh quality, especially for large range of motion and soft tissues attached to bones. Simple geometrical approaches used to position dummies cannot be directly applied to FE HBMs due to the presence of soft tissues. The most common approach used for positioning FE HBMs is to perform a full FE simulation, e.g., in Ls-Dyna (LSTC, USA), between the original and target position. Among alternative approaches, a constraint-based simplified simulation approach was recently proposed and implemented in the PIPER open source software.

In positioning by FE simulation, loads or displacements are applied to move the model to the desired position [1]. The advantage of this approach is the respect of the contacts (although gaps may open in sliding contact formulations) and the absence of inverted elements in simulations that terminate successfully. Besides the difficulty to define the target posture, the process can be time consuming for large models, as significant simulation time may be required to mitigate inertial contributions. Beyond cost, simulations may also lead to artefacts as the initial strains and stresses in tissue are typically not considered, as the biomechanics of the motion is not described. More specifically, *in vivo* postural changes are driven by muscles (muscle contraction or relaxation) pulling on tendons. Such mechanisms are typically not described in the positioning simulations, which can lead to unrealistic folds in tendons, skin, muscles and other soft structures being compressed.

The simplified constraints-based simulation implemented within the PIPER software makes the process more interactive for the definition of the target, and much faster for the model transformation. Based on the SOFA framework (www.sofa-framework.org) [2], this method discretises the inside of a HBM by a regular grid of voxels and performs an implicit iterative constraints-based simulation. The simulation is done on a simplified model, which does not contain all the components of the original FE mesh, but by default only the external skin envelope and the shape of bones. The soft tissues in between are homogenised and transformed by a limited number of interpolation functions. Contacts, collisions and 6 degrees of freedom joints provide a realistic articulation of the skeleton. The simulation is driven by positional and/or angular targets defined for the bones

Tomas Janak is a PhD student in Biomechanics (tomas.janak@ifsttar.fr, tel. +33 4 72 14 26 68), Yoann Lafon, PhD is Assistant Professor and Philippe Beillas, PhD researcher at the LBMC, UMR_T9406, Université Claude Bernard Lyon 1 - Ifsttar in Lyon, France. Philippe Petit, PhD is a Research Engineer at the LAB PSA Groupe - Renault in Nanterre, France.

and joints, and can be interfaced with *a priori* knowledge (e.g., spine curvature predictor [3]). The simulation is interactive which helps to quickly adjust and define a plausible target. That target can be used for positioning by full FE simulation (as previously described) or to transform directly the original model. However, when the simplified simulation is used to transform the original model directly, the simplifications often produce surface (shape) and volume (internal) artefacts which can lead to degraded element quality and inverted elements.

In the end, in both cases (full FE or simplified simulation), the positioned FE HBM can suffer from surface artefacts and/or element quality issues. The surface shape can be manually modified to make it more plausible, e.g. by smoothing or re-modelling it. However, common tools for both 2D and 3D mesh smoothing (i.e., available software such as Ls-Prepost, Mesquite, Cubit, IcemCFD etc.) can typically only act on individual connected components (i.e., they do not account for disconnected components). Therefore, modifying only the boundary of a given component will adversely affect the underlying 3D elements and also can make it penetrate another component. At the same time, smoothing only the internal 3D mesh by fixing the surface may not be sufficient to remove the artefacts.

Overall, there is a need for smoothing approaches to improve the mesh quality of FE HBM after positioning while respecting the internal topology of the model (i.e., be able to smooth across gaps while maintaining them and respecting the bone geometry).

This paper presents a smoothing methodology to improve the mesh quality of HBMs after positioning – either by FE or by simplified simulation – and provides evaluations in three test cases and recommendations for its use. The methodology uses classical surface smoothing (for the skin) as a tool to repair the visible shape degradation. This repaired skin then acts as a boundary constraint for the 3D smoothing of the internal parts of the model. For the internal smoothing, the proposed approach is to smooth the transformation used to change the posture of the model rather than to smooth the positioned mesh directly. A meshless interpolation method, i.e. such that is defined using all the nodes of the model regardless of the underlying mesh, is used to create a smooth transformation field across all components of the model, which is expected to maintain the gaps between disconnected components and limit the element degradation.

II. METHODS

Target pre-processing

The transformation smoothing requires some constraints that define the overall desired shape. For this purpose, the skin surface after positioning was smoothed to obtain a skin that appears plausible (based solely on operator's opinion and experience). Two software tools were used depending on the test case:

- Ls-Prepost (version 4.5, LSTC, USA) surface smoothing, after selecting the regions manually. In some cases when smoothing led to significant shrinking, the offset function was used to enlarge the skin.
- PIPER surface smoothing: the *Crease Detection* tool available in PIPER was used to semi-automatically select the damaged surface areas. The tool compares the dihedral angles between neighbouring elements of the original and positioned model, and selects areas where the change is higher than a user-defined threshold. The selected areas can then be smoothed within PIPER by a surface smoothing tool [4]. However, PIPER does not include the offset function mentioned above, which limits its use to cases where it is not needed.

Transformation smoothing

Interpolation by Kriging has proven to be effective for morphing HBMs [5-10]. The Kriging interpolation function is defined by one set of *control points* (CPs) defined in a source and a target position. It gives the best linear unbiased prediction of the quality (e.g., the position of points) for any point in the source's domain [11] based on the known positions of the CPs. For interpolation of 3D point positions, a method called the Radial Basis Function interpolation leads to equivalent interpolation function as the Dual Kriging formulation [11] used in this paper. Depending on the author, both names can be found in literature referring to the same interpolation. The method also allows non-zero variance to be assigned to the CPs, signifying that the target positions of the CPs are not known exactly. The resulting approximation function is then smoother for the price of only approximating rather than interpolating the CPs positions. This is often called the "nugget" effect [5].

In the current scenario, CPs are defined as nodes on the skin and surfaces of bones, the source corresponds

to the model in the initial (or any intermediate) posture and the target to the model in the final posture. Kriging is used to interpolate the positions of all the nodes of the model. In effect, Kriging replaces the initial positioning transformation of the model. Assuming the interpolation gradient does not vary abruptly between neighbouring CPs, this process preserves the relative positions of individual parts of the HBM, as all of them are morphed by the same, continuous interpolation field. This is expected to help maintaining gaps in contacts.

Test Case 1 and 2: PIPER Child model trunk flexion using PIPER positioning or FE simulation

The first test case uses the PIPER Child model at the 6 years old age (v1.0.0, available online, www.piper-project.org). The model consists of 140,022 nodes and 545,909 elements. The model is positioned using the PIPER positioning tool (module *fine*) and the default application parameters. The motion consists in flexing the trunk and neck forward by 200 mm at the skull (Fig. 1). This leads to surface artefacts (related to the interpolation function) as well as internal element quality issues (e.g., negative volumes) (Fig. 2 top).

The second test case used the same positioning target (saved in PIPER), followed by a FE simulation in LS-DYNA (LSTC, CA) to transform the baseline model. In this approach, beams are attached by one node to each bone surface node and the motion of the free node of the beam is imposed using *BOUNDARY_PRESCRIBED_MOTION_NODE with linear trajectories between the source and target position. For the current application, the motion was decomposed in three steps. This approach was automated by adapting Python scripts provided with PIPER. After the simulation was run (250 ms), significant unrealistic folds were visible in the abdominal region (Fig. 2 bottom).

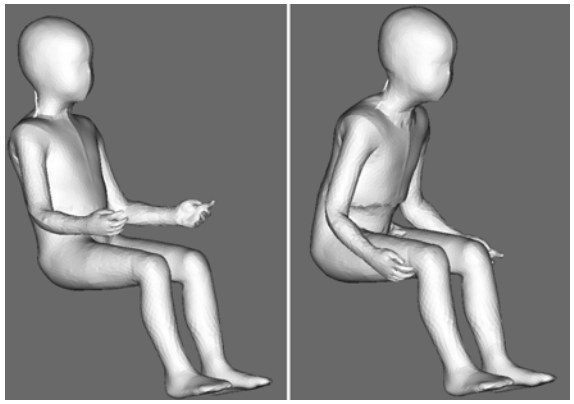

Fig. 1. Test Case 1 – the PIPER Child model in the reference position and after positioning in PIPER. The same target position was used for Test Case 2.

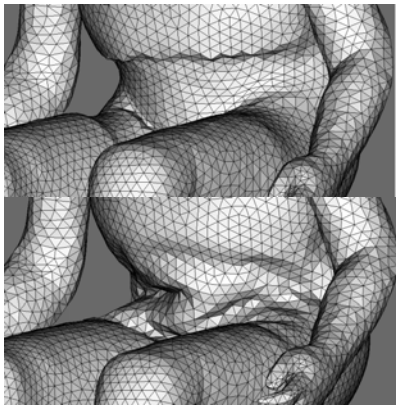

Fig. 2. Test Cases 1 and 2 – surface artefacts below the ribs after PIPER positioning (top) and on the abdomen after FE simulation positioning (bottom).

Test Case 3: GHBMC M50 Detailed motorcyclist position by FE simulation

In the third test case, the GHBMC M50 detailed occupant model (GHBMC M50-O in further text) was equipped with a motorcycle helmet and seated on a motorcycle (Fig. 3). The model is composed of 1,258,012 nodes and 2,294,923 elements. The postural change, performed for another study, required moving the spine, neck, upper and lower extremities such that the position is plausible (including hands on the handle, feet on the pedal, pelvis angle, etc.). That position was defined interactively using the PIPER pre-position module. A full FE simulation was then run in Ls-Dyna, using the same Python scripts as in the second test case. The simulation terminated without error (no negative elements) but skin folds that did not look realistic were visible on the upper thighs, knees and back (Fig. 4).

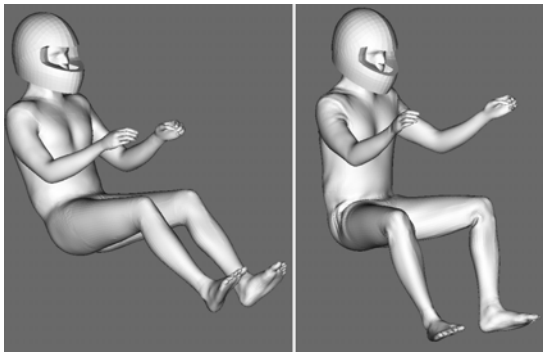

Fig. 3. The GHBMC M50-O with helmet positioned from reference position (left) to motorcyclist (right).

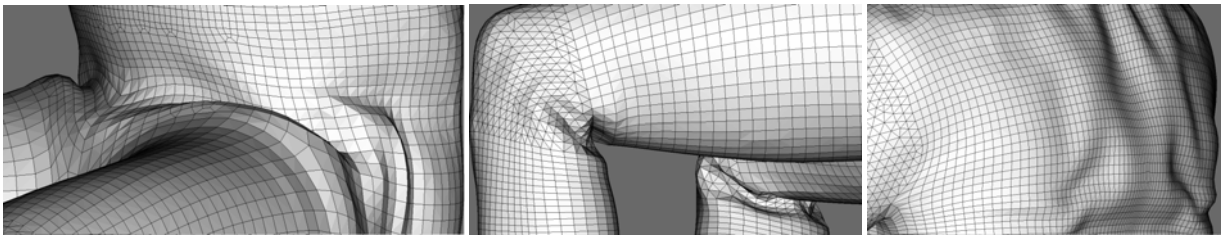

Fig. 4. GHBMC M50-O in motorcyclist position: details of folds at the upper thighs, knees and upper back.

Evaluation Criteria and Implementation

Models were checked for negative volume elements, since those are unsuitable for FE simulation. The normalised determinant of the Jacobian matrix (Scaled Jacobian - SJ) was monitored as a metric of element shape quality. The SJ is 1 for an ideal element (with equilateral sides), and negative for an inverted element [12]. The volumes and SJ of elements were computed in PIPER using the VTK library.

The approach used to smooth the transformation is driven only by surface geometrical targets (bones and skin) and does not put any constraint on other anatomical structures. This means that only internal flesh elements are affected by the transformation smoothing, as the position of skin and bones is predefined by the target geometry. The description of which elements belong to bones and which to skin is stored in "metadata" files, which are available for both used models and PIPER uses them to automatically select the appropriate nodes. The shape or volume of elements could change, which is not desirable as mass conservation is expected in posture change [13]. The volume of solid elements before positioning, after positioning and after transformation smoothing was therefore measured in Ls-Prepost.

Transformation smoothing was implemented into PIPER. The smoothing can be limited to a specific area by selection boxes defined by the user. The PIPER implementation of Kriging includes algorithms that allow processing any number of control points. It also includes an optional nugget parameter defined at each control point [5] to increase the smoothness of the transformation by violating the target position. The implementation is available in the version 1.0.2 of the PIPER software (except for the volume calculation). Tests were performed on a PC with Intel Xeon E5-1650 CPU (3.5 GHz, 6 cores), 32 GB RAM and Windows 7 64-bit operating system.

III. RESULTS

Test case 1: Pre-processing: surface smoothing

The skin surface was smoothed near the lower ribcage, thighs and around the waist (Fig. 5). The regions were selected as a single action using the PIPER *Crease Detection* tool, and then the selected surface elements were smoothed in PIPER. The whole process lasted less than two minutes. The positioned model contains 591 negative volume elements after the PIPER positioning. After the surface smoothing, this number did not change.

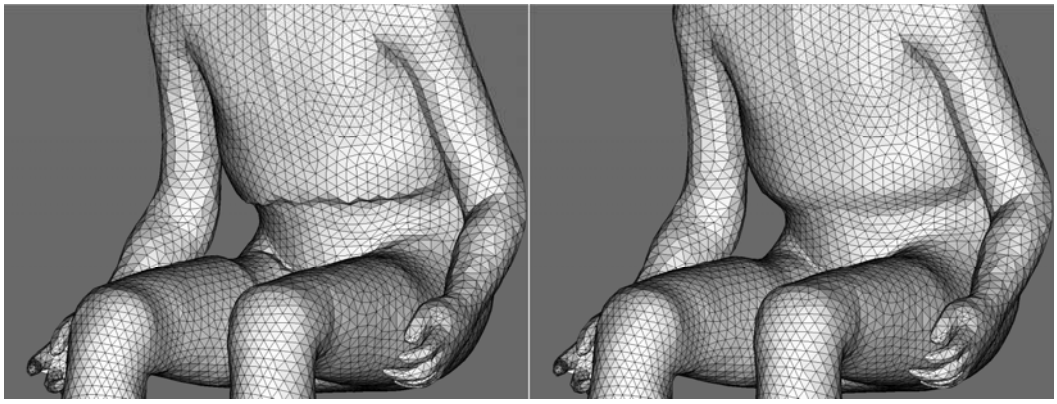

Fig. 5. Surface of the PIPER Child model after PIPER positioning (left) and after PIPER surface smoothing (right).

Transformation smoothing

The negative volume elements were along the cervical and thoracic spine, bottom of ribcage and pelvis. Since the quality of the model after positioning was not degraded elsewhere, only the torso was selected for smoothing. At first, small selection boxes were tightly defined around the regions with negative volumes (Fig. 6 – left). Transformation smoothing was applied using the baseline model as source and positioned with smoothed surface as target. However, this resulted in artefacts and insufficient smoothing (Fig. 6 – middle).

An alternative selection box enclosing the whole trunk and head was then defined (Fig. 6 – right). Using this larger box, three adjacent negative volume elements remained after smoothing, located next to one cervical vertebra. They were fixed in Ls-Prepost using the node reordering function (Check menu). The smoothing took 5 minutes 3 seconds to compute with 37,802 control points. Using a nugget did not improve the result. The no load simulation ran without error. The number of elements with negative SJ increased from two in the baseline model to 492 after positioning, 618 after skin smoothing and decreased to 19 after transformation smoothing (Fig. 7).

Regarding the volume changes, the solid elements represent a volume of 16,339 cm^3 in the baseline, 16,271 cm^3 after positioning, 16,269 cm^3 after skin smoothing and 16,288 cm^3 after transformation smoothing, which makes a variation of less than 0.5% between the initial and final postures.

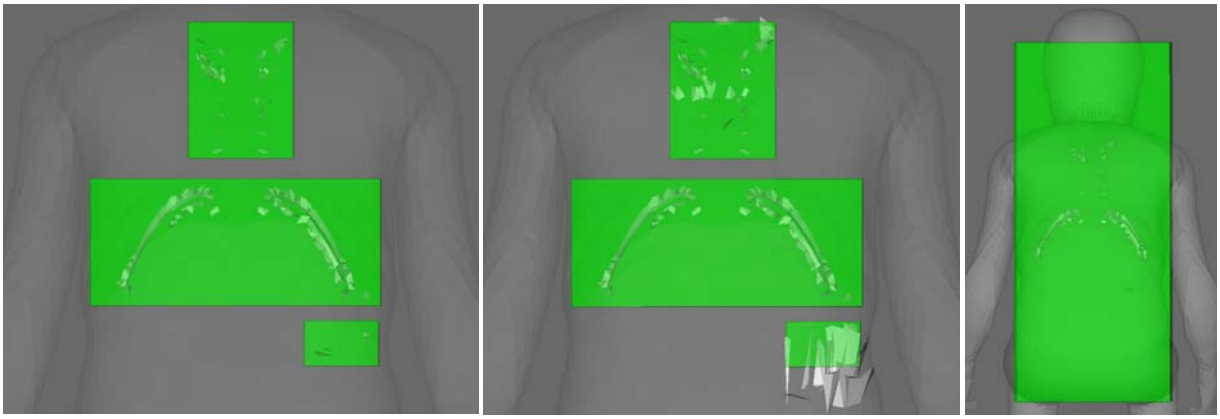

Fig. 6. Test Case 1 - Torso of the child model before (left) and after (middle) transformation smoothing for very tight selection of smoothing areas (green boxes, spanning the entire depth of the body, anterior to posterior. Negative volume elements are drawn as solid; the model outline is drawn as semi-transparent. Too localised selection areas did not remove the existing negative volume elements and even created new ones. Right: final area selected for transformation smoothing by Kriging.

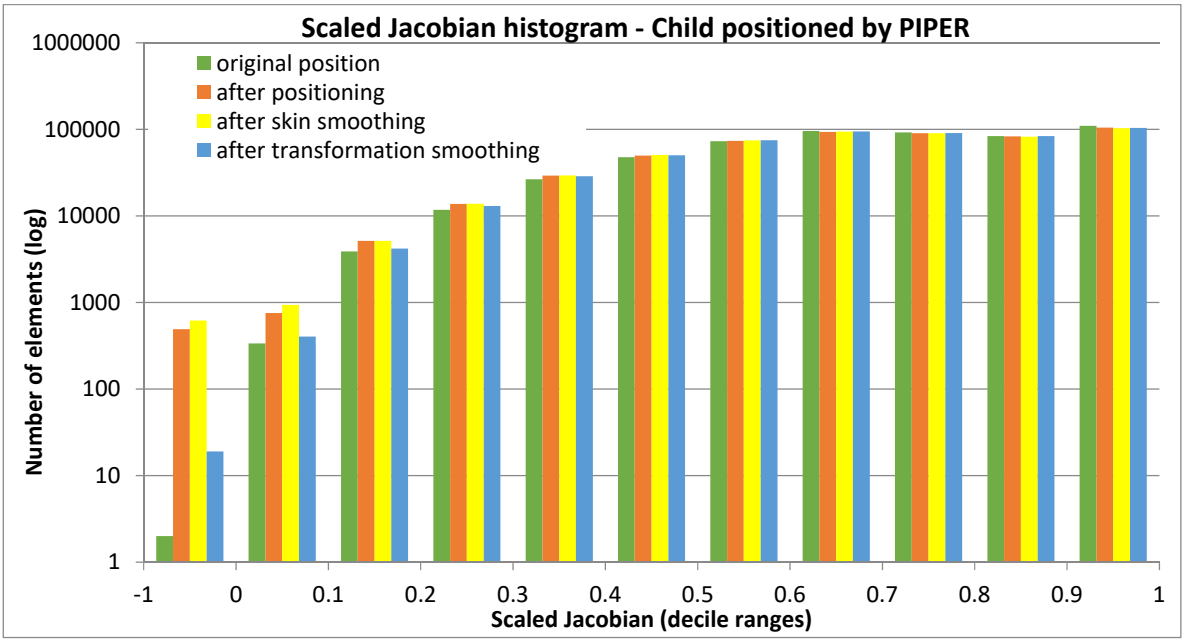

Fig. 7. Test Case 1 – Histogram of SJ of elements at each step of the process (logarithmic scale). The histogram groups elements by deciles for positive values and all negative values to one group. Note that the two elements from the baseline model have a negative SJ (i.e., a non-positive SJ at one integration point), but maintain positive volume as a whole.

Test case 2: Pre-processing: surface smoothing

After child positioning by FE simulation, skin artefacts were mainly present around the waist and the abdomen. The skin was smoothed using crease detection and surface smoothing in PIPER, as for Test Case 1 (Fig. 8).

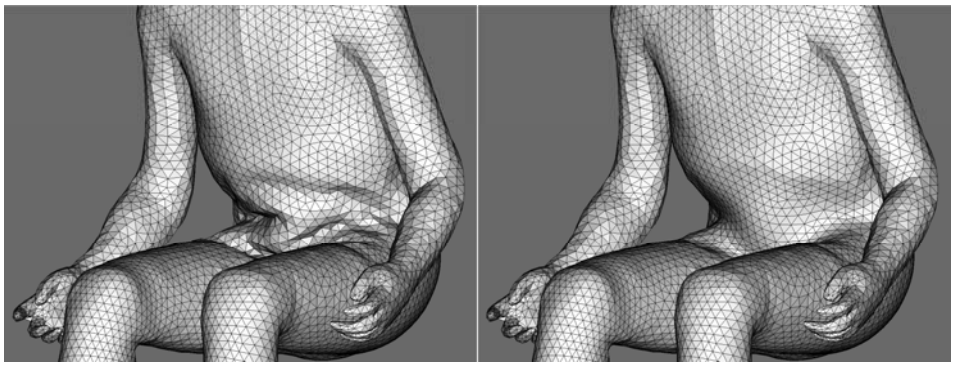

Fig. 8. Surface of the PIPER Child model after positioning by FE simulation (left) and after PIPER surface smoothing (right).

Transformation smoothing

Smoothing the surface of the skin had only limited effect on element quality but changed the relative thickness of the superficial solid layer (flesh/fat component) versus the abdominal muscle layer (Fig. 9).

Transformation smoothing was applied using the model after FE simulation as source, and the model with the smoothed surface as target. The smoothing area was defined by a selection box only around the abdomen (anterior-to-posterior). The thickness of the two superficial layers after the transformation smoothing was more homogenous than after surface smoothing (Fig. 9d). The transformation affected part of the liver (located between the skin surface and bones). The volume of solid elements after positioning was 16,071 cm^3 and 15,986 cm^3 after smoothing. Both volumes are lower than the baseline (16,339 cm^3) by around 2%. Transformation smoothing cancelled the quality degradation introduced by surface smoothing (Fig. 10).

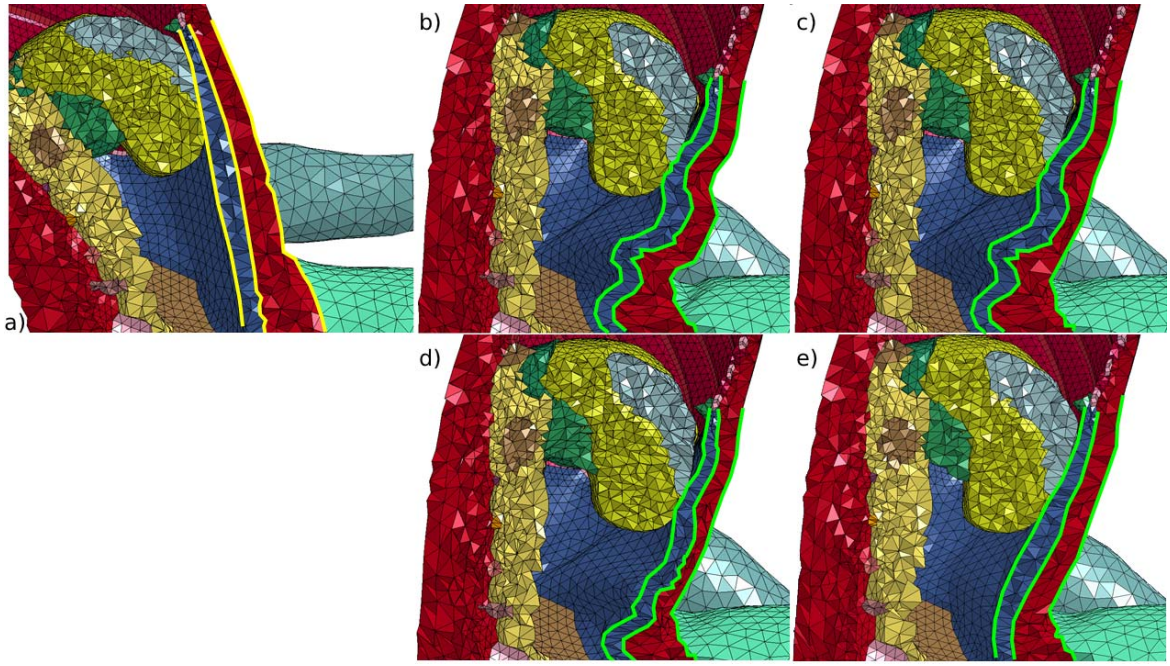

Fig. 9. Test Case 2 - Section through the PIPER Child model torso. (a): model in original position, (b): after positioning by FE simulation, (c): after smoothing the skin of the abdomen. The bottom row shows the result after applying transformation smoothing – (d): using the FE positioned model as a source, (e): the original position as a source. Overlay lines identify the external, medial and internal boundary of the fat and muscle layers on the abdominal wall, in the initial model (yellow lines) and for other steps (green lines).

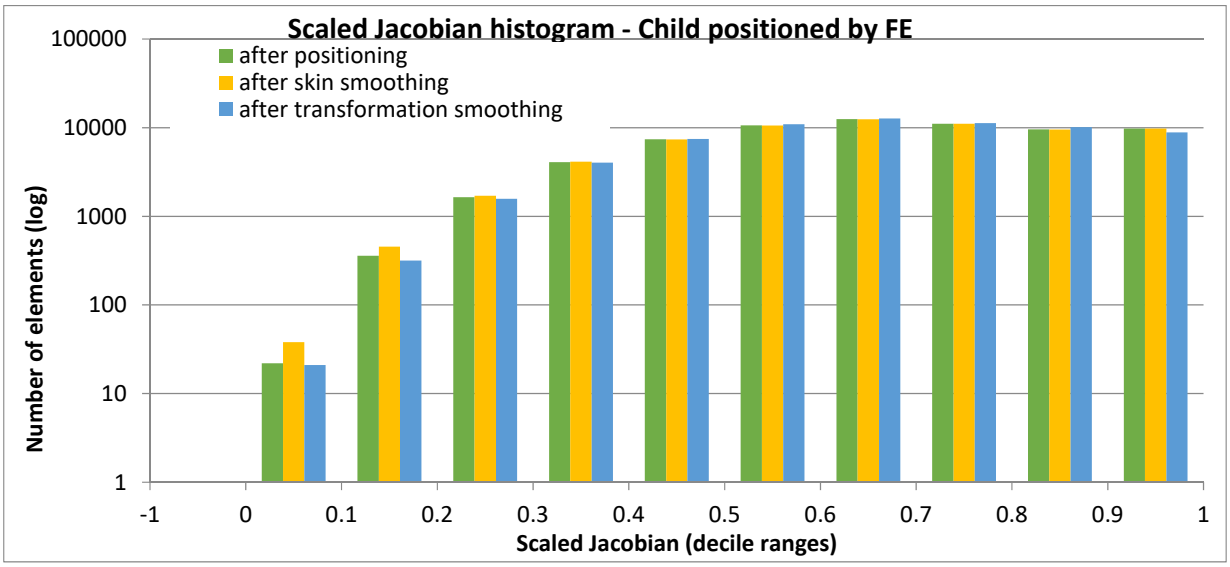

Fig. 10. Test Case 2 - Histogram of SJ of elements at each step of the process (logarithmic scale). The histogram groups elements by deciles for positive values and all negative values to one group. Only elements around the waist and the abdomen were measured in order to get a better contrast of values.

As an alternative, the transformation smoothing was applied using the original position as source instead of the already positioned model. That approach led to even smoother abdominal wall (Fig. 9e) and only marginal differences in SJ distribution for higher deciles. The resulting model had no negative volume elements and a volume of 16,111 cm^3. When compared to the first test case – which also used the original position as source – there were slightly more low quality elements (488 vs. 423 elements with SJ < 0.1).

Test case 3: Pre-processing: surface smoothing

In the GHBMC M50-O positioned in motorcyclist posture by FE simulation, the main visible folds were near the upper thighs, upper back and knees. The crease detection PIPER algorithm was able to select these regions, but the PIPER smoothing did not result in a satisfactory correction. The regions were therefore selected manually and smoothed in LS-Prepost. Mesh offset was used to compensate for shrinking when needed. Fig. 11 shows details of the three areas before and after the surface smoothing. The process lasted for about 15 minutes as it required more manual input, mainly for offsetting skin after smoothing it.

While the GHBMC M50-O model did not contain any negative volume elements after positioning, the surface smoothing created 145 of them in the superficial solid element layer just below the skin.

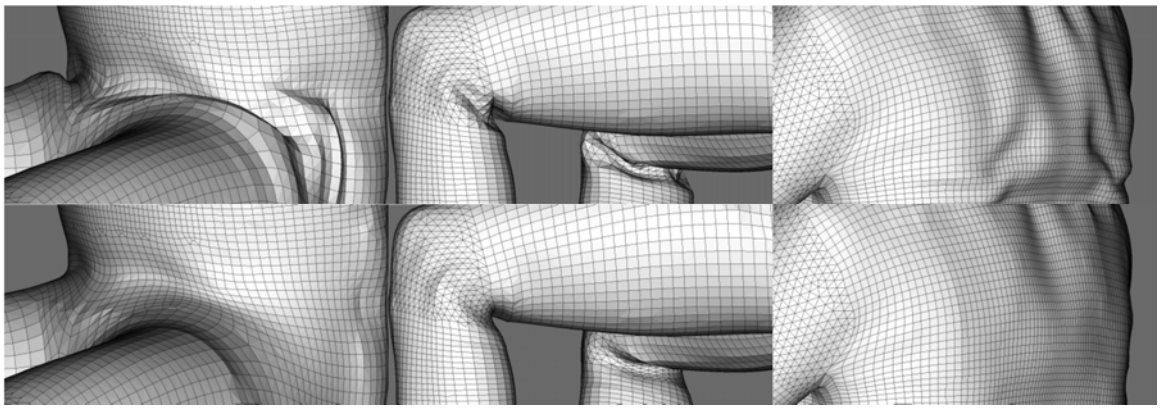

Fig. 11. Surface of the GHBMC M50-O model's upper thighs (left), knees (middle) and back (right) after positioning by a FE simulation (top) and after surface smoothing (bottom).

Transformation smoothing

Transformation smoothing was applied using the model after FE simulation as source, and the model with the smoothed surface as target. Three selection boxes were created in the areas that were smoothed (Fig. 12). The runtime was 4 minutes 59 seconds.

Transformation smoothing removed all negative elements introduced by the surface smoothing and as in the second test case it recovered the element quality after positioning by simulation (Fig. 13) by homogenising the thickness on the superficial layers near the smoothed surfaces (Fig. 14).

The volume of all solid elements was 70,320 cm^3 in the baseline model, 69,911 cm^3 after positioning (reduction of 0.6%), 69,646 cm^3 after skin smoothing and 69,594 cm^3 after transformation smoothing.

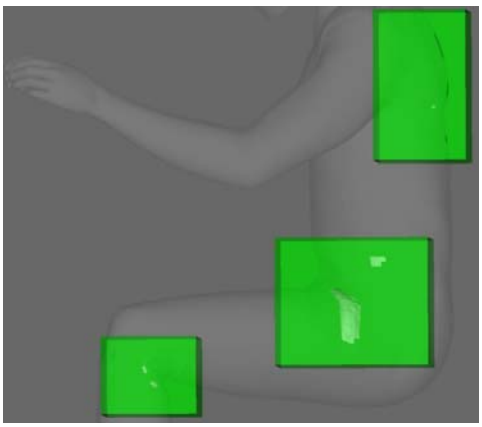

Fig. 12. Test case 3 - Areas selected for transformation smoothing of the GHBMC M50-O after surface smoothing. Selected areas are depicted by the green boxes (spanning through the entire width of the body), negative volume elements are drawn as solid geometry inside the boxes; the outline of the model is drawn as semi-transparent.

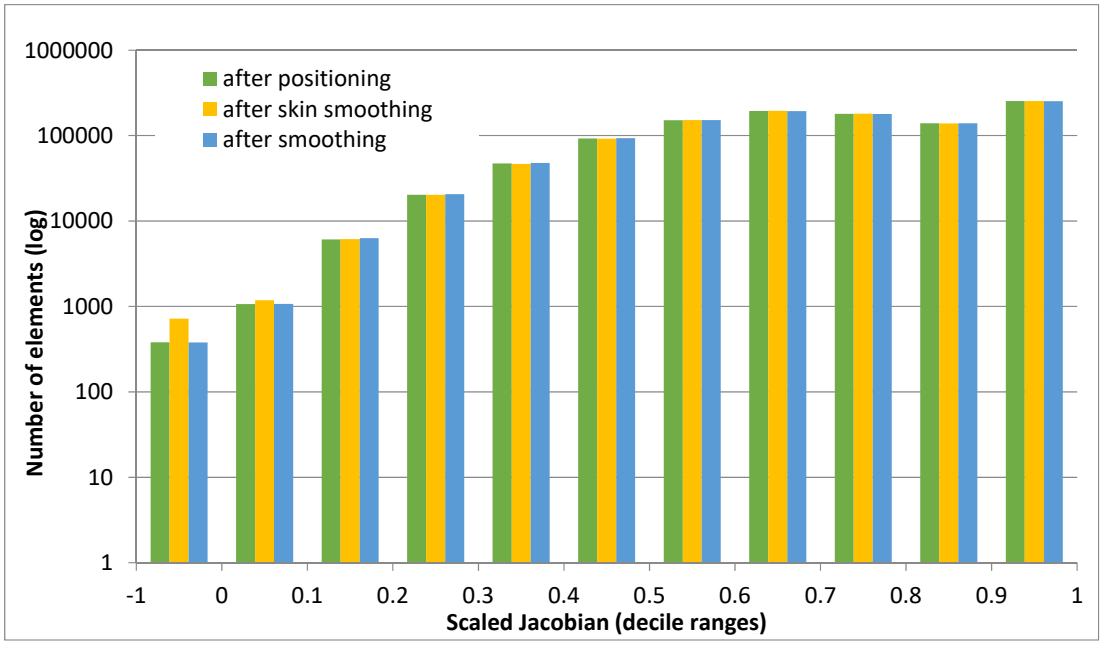

Fig. 13. Test Case 3 - Histogram of SJ of elements at each step of the process (logarithmic scale). The histogram groups elements by deciles for positive values and all negative values to one group. Quality was only assessed in the areas selected for correction in order to get better contrast between values.

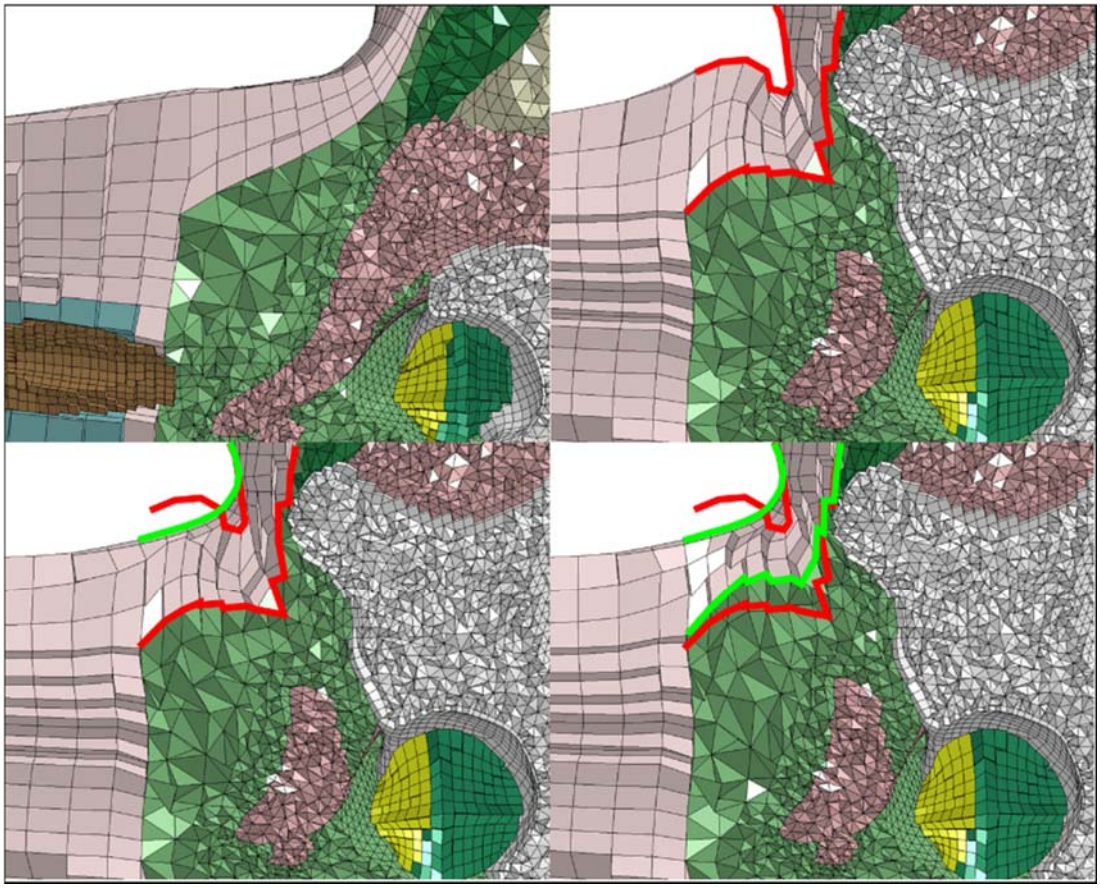

Fig. 14. Test Case 3 - Section through the GHBMC M50-O model left the femoral head: in original position (top left), after positioning by FE simulation (top right), after smoothing the skin (bottom left) and after applying transformation smoothing (bottom right). Overlay lines highlight the superficial layers of solid elements after FE simulation (red lines), surface smoothing (one green line) and transformation smoothing (green lines).

IV. DISCUSSION

This study focused on methodology and software to help smooth FE HBM after positioning. More generally, the methodology can be used to replace the internal transformation between two states of a model. In the current study, the transformation smoothing was applied in combination with surface smoothing to three test cases on two different models, and two positioning usage scenarios (e.g., smoothing of surface artefacts after positioning, internal transformation smoothing after positioning).

In all three test cases, the transformation smoothing improved the element quality while keeping the bones unchanged (which is essential for positioning). An important property of the Kriging method used for the transformation smoothing is that it is meshless, i.e. it defines the transformations based only on the nodes, regardless of their connectivity. As a result, the created transformation field is smooth across all components of the model. The practical implication of that is that the gaps in the model are maintained. Note that it can be expected that other interpolation methods used in place of Kriging would achieve similar results, as long as they share this property. While no quantitative assessment of the gap changes was performed, no issues related to initial penetrations were observed after the Ls-Dyna simulations without loading.

For the positioning using PIPER, negative volume elements were almost completely removed (only three left in Test Case 1, removed by reordering the nodes). This issue typically arises around bones and joints (e.g., spine, shoulder joint) where soft tissues are in the vicinity of several bones (constraints) moving in different directions. This creates a high gradient in the transformation field which may result in negative volumes. In effect, the transformation smoothing, if using bone and skin for CPs, is not able to simulate sliding. This may be the main limitation of the proposed approach. One countermeasure could be to use capsules or other anatomical structures that can slide as constraints instead of the bones. This may require significant efforts beyond the current implementation although capsule modelling is already possible within PIPER positioning. One must also note that this issue of high gradient may be present in FE simulations too when the soft tissues are attached to bones using tied contacts. While only one test case of this positioning scenario was presented, it is believed that it is fairly representative based on the current experience with the smoothing approach (ability to remove most negative volumes, with a few left at most, and none for small range of motion).

For the smoothing after positioning by FE simulation, the proposed approach also showed the ability to correct surface artefacts and re-interpolate the internal deformation to homogenise elements in the superficial tissue layers after the surface smoothing.

While the results of the transformation smoothing seemed visually plausible, the assessment of the physiological realism of the transformation was not evaluated. The effect of the transformation smoothing on the overall volume was limited, as expected by the fact that the skin is used as a constraint. When comparing the test cases, while the PIPER positioning approach does not ensure conservation, it led to better volume conservation than positioning by FE simulation. However, the respect of internal geometry (e.g., ligament section) was not assessed. This should be investigated in the future, comparing specific anatomical structures (e.g., ligaments) transformed by simulation (with possible artefacts due to folding) or geometrical interpolation. This would help define the need for additional internal constraints in the smoothing to prevent volume changes or correct for positional changes (e.g., [13]).

Beyond internal interpolation, the assessment of the realism of the external shape of the models after positioning was beyond the scope of the study. Folds and corrections were defined manually as the study focused on numerical smoothing approaches. While it may be subjective, significant artefacts could be observed in all test cases, some of which may affect the model response in subsequent simulations if the initial strains and stresses are zeroed. External surface measurements performed during positional changes would be useful for such analyses. A study on the effect of positional changes on the shape of the thigh-abdomen junction in obese subjects is under preparation to help with future methodological evaluations.

Future assessments should include full simulations to quantify the effect of different positioning and smoothing approaches not only on the geometry but also on the impact response: while the SJ distribution after transformation smoothing was similar for many deciles to the baseline model, the effect on the model stability and local response is still unknown.

In terms of implementation, the current transformation smoothing is now part of the PIPER framework and is available online as open source software. The only requirement to apply smoothing to two states of the same model is the ability to import the model in PIPER, and to have metadata files defining anatomical structures that

will be used as constraints (bones, skin). The smoothing is relatively fast (a few minutes) when only part of a HBM is selected. By experience, this can increase to 20 to 30 minutes for the full GHBMC M50-O on the PC configuration listed above.

In terms of recommendations, one important observation is the need to define a large enough selection box: the interpolation field defined by CPs only within the selection box should ideally be equal to an interpolation field that would be defined by using all nodes of the HBM as CPs. It would ensure smooth transition between the transformations (and hence the resulting mesh) inside and outside of each box. While the perfect equality of those fields will almost never be achieved, choosing a box that extends significantly far beyond problematic regions (the ones that need to be smoothed) will minimise the difference between the ideal, global, transformation and the local one within the box. The use of a nugget, which can be highly beneficial in some other contexts [5] was not found to be helpful in the current scenario. This may be due to the fact that the nugget parameter can only be used for the skin CPs (as the bone shape needs to be kept intact in the positioning scenario), and that negative volume issue seems to remain in regions with relative bone motion. The effect on using a small nugget to let bone deform in these regions has not been assessed yet.

As was shown on Test Case 2, the previous state prior to transformation smoothing can be either the original baseline model or the results of the FE simulation. The two approaches can provide significantly different results. The choice of initial state is likely to be dependent on the anatomical region and the positioning scenario: while using the original baseline for source could help with mesh quality in the interpolation, replacing the positioning by FE transformation may result in issues near joints for large range of motion (already discussed). For these cases, using the intermediate state as source may be preferred.

Regarding the surface preparation, crease detection was useful to quickly help select the areas with folds and creases. The PIPER software limitation was more apparent for the surface smoothing in the case of the GHBMC M50-O, particularly on the back and knees, where the skin component is relatively thin. In those parts, smoothing lead to penetration of underlying components and PIPER currently lacks the tools to manually re-model them (offset). This should be further investigated as different smoothing algorithms may not suffer from such problems. For example, algorithms based on manifold harmonics [14] or diffusion flow fairing [15] could be investigated, as they promise solutions that prevent shrinking. In the meantime, a partial import and export of a selected region through a scripting interface is possible to easily edit it outside PIPER.

If coupled with a reliable surface smoothing algorithm, crease detection could be useful for fully automated correction of positioning surface artefacts. The automation of the transformation smoothing process is also considered in the future. Currently, it is possible to fully automate the process, but only if the whole model is smoothed, which can take tens of minutes. To exploit PIPER's ability to perform localised Kriging to lower the computational cost, an algorithm for automatic creation of boxes – either around creases or negative elements – is needed. A prototype using clustering techniques was designed but it does not work yet in cases where the negative volume elements are scarce as it creates boxes that are too small and too numerous. Also, a reliable heuristic for assessing the size of the boxes such that they are large enough to ensure well-defined transformation field (as discussed above) would have to be developed. Besides helping with the automation of positioning workflow, the smoothing automation would help with a systematic quantification of the smoothing effects on the model response.

Fig. 15 expresses the workflow for transformation smoothing presented in this paper as a flowchart. Apart from the recommendations already mentioned above, the flowchart shows an additional one: if there are multiple damaged areas, it might be worthwhile to perform the transformation smoothing separately per each area. Since PIPER stores the state of the mesh after each operation that modifies it, this approach allows the user to undo the smoothing of each damaged area separately if it did not yield the desired quality (e.g. because the target needs to be improved), without having to undo smoothing on all other areas. Lastly, note that while the target pre-processing for the presented test cases was done only on the skin, in general it can be done on any target if needed (bones or even other parts if they are used as target) or not at all if the positioning method damages only the internal parts. Hence the flowchart specifies only "surface targets" rather than "skin target".

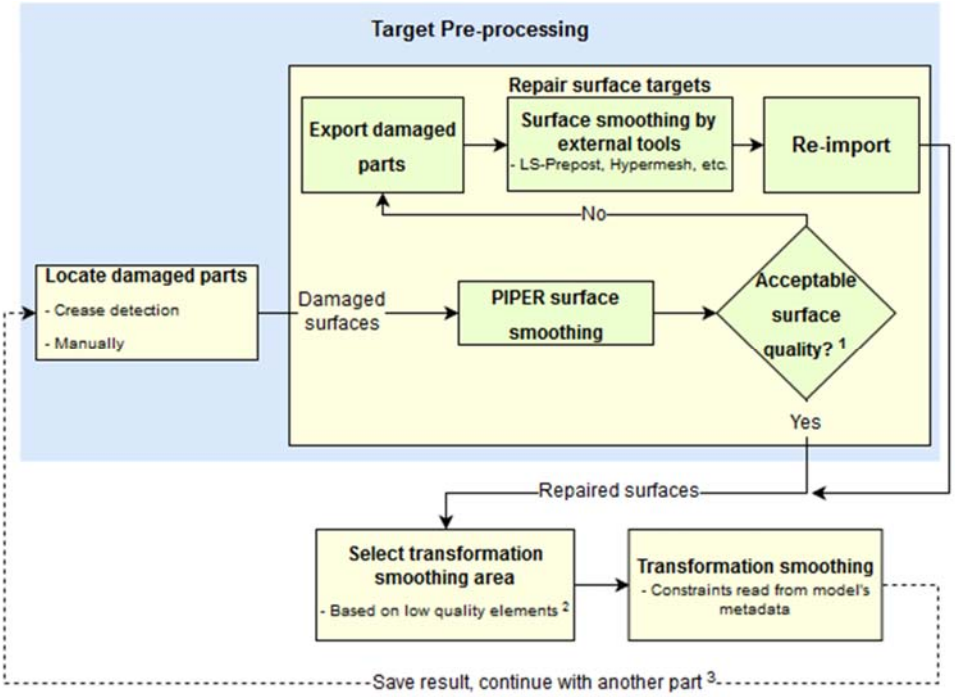

Fig. 15. Workflow for transformation smoothing. Recommendations for some of the step (marked by numbers in the flowchart): (1): what is considered acceptable quality will differ based on the application, but at least the user should make sure that target surfaces will not penetrate each other. (2): ensure that the smoothing area is extended significantly beyond the low quality elements to ensure smooth transition between smoothed and unsmoothed parts. (3): if there are multiple separate damaged areas, smoothing per parts might be more convenient to be able to undo them one by one if needed.

V. CONCLUSIONS

This study proposes a new workflow to efficiently smooth HBMs after they have been positioned while maintaining gaps between anatomical structures. The proposed technique succeeded in providing a runnable mesh after positioning in the three test cases selected for this study. It improved significantly the mesh quality while reducing undesired skin surface artefacts and removing negative volume elements. The correction was achieved in a reasonable computation time, from a few seconds for a small region to a few minutes. The approach also requires minimal user input as some actions can be automated. The method reported in this paper, as well as the proposed workflow, is readily implemented in the PIPER open source framework, which is freely available online.

The crease detection functionality in PIPER has proven useful in detecting typical positioning artefacts on the skin. However, the surface smoothing tools available in PIPER were insufficient for pre-processing the skin of the GHBM M50-O as the thickness of the skin component is relatively small and modifying it often results in penetrations with other components. Software with more advanced smoothing algorithms than PIPER could be preferable for pre-processing of the skin target. Once experience is gained on these algorithms, it might be beneficial to implement them in the PIPER software.

For most of the evaluated positioning scenarios, the HBM in final posture corrected by transformation smoothing was runnable. Issues appear where only a small number of elements were subjected to multiple moving constraints (e.g., soft tissues near moving vertebrae, sliding transformation) as such high gradient deformations are difficult to capture with the proposed approach: in such cases the approach could fail to remove negative volume elements. While the reported transformation smoothing requires a baseline model with initial consistent element quality (no negative volume elements), it is independent of the positioning approach (here PIPER tool or FE simulation) as well as the topology of the HBM (type of interaction between anatomical structures). Presently the method does not ensure the preservation of the volumes of internal structures, but future efforts should include work on constraints for the shape of the skin (e.g., around joints) or inside to correct the position of organs and to control the volume changes.

The realism of the solution after positioning should be evaluated before examining alternative deformation

methods like skinning techniques: experimental work on positional changes regarding obesity is under preparation. More generally, the effect of the positioning approaches and smoothing on the response of positioned HBM should be evaluated.

VI. ACKNOWLEDGEMENT

Authors would like to thank Marie-Christine Chevalier (Ifsttar) for providing the positioned GHBMC M50-O motorcyclist model (French project Secu2RM).

VII. REFERENCES

[1] Poulard D, Subit D, Donlon J–P, Kent R W. Development of a computational framework to adjust the pre-impact spine posture of a whole-body model based on cadaver tests data. *Journal of Biomechanics,* 2015, vol. 48(4):pp.636–643.

[2] Tournier M, Nesme M, Gilles B, and Faure F. Stable Constrained Dynamics. *ACM Transactions on Graphics (TOG) - Proceedings of ACM SIGGRAPH 2015*, 2015, vol. 34(4):pp.132:1–132:10.

[3] Fréchède B, Gardegaront M, Lemaire T, Wang X, Beillas P. Design of a physiological spinal posture predictor in the PIPER project. *Conference Proceeding of the XXVI Congress of the International Society of Biomechanics (ISB)*, 2017, Brisbane, Australia.

[4] Taubin G, Zhang T, Golub G. Optimal surface smoothing as filter design. *ECCV '96 Proceedings of the 4th European Conference on Computer Vision-Volume I - Volume I*, April 15 – 18, 1996, pp.283-292.

[5] Jolivet E, Lafon Y, Petit P, and Beillas P. Comparison of Kriging and Moving Least Square Methods to Change the Geometry of Human Body Models. *Stapp Car Crash Journal*, 2015, vol. 59:pp.337–357.

[6] Vavalle N A, Schoell S L, Weaver A A, Stitzel J D, Gayzik F S. Application of Radial Basis Function Methods in the Development of a 95th Percentile Male Seated FEA Model. *Stapp Car Crash Journal*, 2014, vol. 58:pp.361–384.

[7] Hu J, Fanta A, Neal M O, Reed M P, and Wang J-T. Vehicle Crash Simulations with Morphed GHBMC Human Models of Different Stature, BMI, and Age. *Proceedings of the 4th International Digital Human Modeling Conference*, 2016, Montreal, Canada.

[8] Hwang E, Hallman J, Klein K, Rupp J, Reed M, Hu J. Rapid Development of Diverse Human Body Models for Crash Simulations through Mesh Morphing. *SAE Technical Paper 2016-01-1491*, 2016.

[9] Beillas P, Berthet F. An investigation of human body model morphing for the assessment of abdomen responses to impact against a population of test subjects. *Traffic Injury Prevention*, 2017, vol. 18(sup1):pp.S142–S147.

[10] Guleyupoglu B, Koya B, Gayzik FS. Leveraging Human Body Models of Varying Complexity for Computational Efficiency. *61st STAPP Car Crash Conference,* 2017, Charleston, South Carolina, USA.

[11] Trochu F. A contouring program based on dual kriging interpolation. *Engineering with Computers*, 1993, vol. 9(3):pp.160–177.

[12] Knupp P M. Achieving finite element mesh quality via optimization of the Jacobian matrix norm and associated quantities. Part II – A framework for volume mesh optimization and the condition number of the Jacobian matrix. *International Journal for Numerical Methods in Engineering*, 2000, vol. 48(8):pp.1165–85.

[13] Beillas P, Lafon Y, Smith F W. The effects of posture and subject-to-subject variations on the position, shape and volume of abdominal and thoracic organs. *Stapp Car Crash Journal*, 2009, vol. 53:pp.127-154.

[14] Vallet B, Lévy B. Spectral Geometry Processing with Manifold Harmonics. *Computer Graphics Forum*, 2008, vol. 27: pp.251-260.

[15] Desbrun M, Meyer M, Schröder P, Barr A H. Implicit fairing of irregular meshes using diffusion and curvature flow. In *Proceedings of the 26th annual conference on Computer graphics and interactive techniques* (SIGGRAPH '99), 1999, New York, NY, USA.